Relationship between electrostatics and redox function in human thioredoxin: Characterization of pH titration shifts using two-dimensional homo- and heteronuclear NMR

ARTICLE *in* BIOCHEMISTRY · MAY 1992

Impact Factor: 3.02 · DOI: 10.1021/bi00128a019 · Source: PubMed

3 AUTHORS, INCLUDING:

G. Marius Clore
National Institutes of Health
550 PUBLICATIONS **59,952** CITATIONS

SEE PROFILE

Relationship between Electrostatics and Redox Function in Human Thioredoxin: Characterization of pH Titration Shifts Using Two-Dimensional Homo- and Heteronuclear NMR†

Julie D. Forman-Kay, G. Marius Clore,* and Angela M. Gronenborn*

Laboratory of Chemical Physics, Building 2, National Institute of Diabetes and Digestive and Kidney Diseases, National Institutes of Health, Bethesda, Maryland 20892

Received November 19, 1991; Revised Manuscript Received January 9, 1992

ABSTRACT: The electrostatic behavior of potentially titrating groups in reduced human thioredoxin was investigated using two-dimensional (2D) ^1H and ^{15}N nuclear magnetic resonance (NMR) spectroscopy. A total of 241 chemical shift titration curves were measured over the pH range of 2.1–10.6 from homonuclear ^1H–^1H Hartmann–Hahn (HOHAHA) and heteronuclear ^1H–^{15}N Overbodenhausen correlation spectra. Nonlinear least-squares fits of the data to simple relationships derived from the Henderson–Hasselbalch equation led to the determination of pK_as for certain isolated ionizable groups, including the single histidine residue at position 43 (pK_a = 5.5 ± 0.1) and a number of aspartic and glutamic acid carboxylate groups. Many of the titration curves demonstrate complex behavior due to the effects of interacting titrating groups, the long range of electrostatic interactions through the protein interior, and, perhaps, pH-induced conformational changes on the chemical shifts. Unambiguous assignment of the pK_as for most of the 38 potentially ionizing groups of human thioredoxin could therefore not be made. In addition, there was no clear evidence that Asp-26 titrates in a manner corresponding to that observed in the *Escherichia coli* protein [Dyson, H. J., Tennant, L. L., & Holmgren, A. (1991) *Biochemistry 30*, 4262–4268]. The pK_as of the active site cysteines were measured, however, with Cys-32 having an anomalously low value of 6.3 ± 0.1 and that of Cys-35 between 7.5 and 8.6. These pK_as are in agreement with proposed mechanisms for redox catalysis of thioredoxin and previously measured pK_as within the active site of *E. coli* thioredoxin [Kallis, G. B., & Holmgren, A. (1980) *J. Biol. Chem. 255*, 10261–10265]. The stabilization of a thiolate anion at physiological pH can be explained by the interaction of the S^γ of Cys-32 with the amide of Cys-35 observed in the previously determined high-resolution solution structure of reduced human thioredoxin [Forman-Kay, J. D., Clore, G. M., Wingfield, P. T., & Gronenborn, A. M. (1991) *Biochemistry 30*, 2685–2698].

Determinations of the ionization constants or pK_as of histidines were among the earliest applications of nuclear magnetic resonance (NMR)[1] spectroscopy to the understanding of the behavior of proteins. Because of the important role of electrostatic interactions in many of the functions of proteins, the ability to assign a pK_a to a specific ionizable group in the molecule (based on chemical shift changes as a function of pH) can aid in the development of mechanistic descriptions of catalysis, binding, and other behavior. Two-dimensional ^1H NMR has been used to determine pK_as of a majority of the aspartate and glutamate side-chain carboxylates of bull seminal inhibitor IIA (Ebina & Wüthrich, 1984) and, more recently, the pK_as for all of the ionizable groups within the pH stability range of mouse epidermal growth factor (Khoda et al., 1991). It is therefore of considerable interest to apply this approach to a protein whose biological activity relies on chemistry involving the ionization of titrating groups.

One such protein is thioredoxin, a small ubiquitous redox-active disulfide/dithiol catalyst, which has been shown to have a variety of functions in the thiol chemistry of the cell (Holmgren, 1989). The proposed mechanism of action of the protein involves the nucleophilic attack by the Cys-32 thiolate anion on a disulfide-containing substrate, producing a mixed-disulfide intermediate, which is further attacked by the thiolate of Cys-35 to yield a reduced substrate (Kallis & Holmgren, 1980). In this work, both 2D ^1H–^1H homonuclear and heteronuclear ^{15}N–^1H experiments have been performed on reduced human thioredoxin, relying on the previous ^1H (Forman-Kay et al., 1989) and ^{15}N (Forman-Kay et al., 1990) resonance assignments and the solution structure determination (Forman-Kay et al., 1991a), to probe the ionization constants of titrating groups in the active site, as well as in the rest of the protein. The present study is aimed at providing clues for a global understanding of the electrostatic behavior of the active form of this redox catalyst and suggests that pH-dependent structural changes and long-range electrostatic interactions due to buried charges can result in complications to a simplistic analysis of chemical shift titration curves.

The pK_a of a free cysteine is 8.3 in aqueous solution (Cantor & Schimmel, 1980), but, since most cysteine residues in proteins are at least partially buried due to their hydrophobic nature, their apparent pK_a could be much higher. The active site cysteine sulfhydryls in human thioredoxin are both around 20% surface accessible in the NMR solution structure (Forman-Kay et al., 1991a), suggesting that their pK_as might be shifted to higher pH values. Chemical modification and fluorescence studies of reduced *Escherichia coli* thioredoxin, however, have indicated that Cys-32 has an anomalously low pK_a (~6.7), stabilizing the thiolate at physiological pH (Kallis

† This work was supported by the Intramural AIDS Targeted Antiviral Program of the Office of the Director of the National Institutes of Health (G.M.C. and A.M.G.).

[1] Abbreviations: COSY, two-dimensional correlated spectroscopy; DTT, dithiothreitol; HOHAHA, homonuclear Hartmann–Hahn spectroscopy; NMR, nuclear magnetic resonance.

& Holmgren, 1980; Reutimann et al., 1981). Dyson et al. (1991) have applied 2D ^{1}H NMR to the determination of pK_as within the active site of *E. coli* thioredoxin, obtaining results showing one pK_a of 7.1–7.4 and another greater than 8.5. The assignment of these ionization constants is somewhat unclear, but there is evidence for the *E. coli* protein that Cys-32, as well as Asp-26, titrate around a pK_a of 7, with Cys-35 having the higher pK_a.

No clear structural rationalization has been found, as yet, for the stabilization of the Cys-32 thiolate in *E. coli* thioredoxin. Early speculation prior to the solution of the X-ray crystal structure of the oxidized form pointed to the role of the ϵ-amino group of Lys-36 in charge stabilization. Data from mutagenesis (Gleason et al., 1990), structural studies of the oxidized form (Holmgren et al., 1975; Katti et al. 1990), and more recent structural work on reduced thioredoxins (Dyson et al., 1990; Forman-Kay et al., 1991a), however, revealed that this was unlikely. Dyson et al. (1990) suggest that the ϵ-amino group of Lys-57 in *E. coli* thioredoxin and the side-chain carboxyl group of Asp-26 may play a role in proton-transfer reactions associated with the redox function, indirectly stabilizing the Cys-32 thiolate. While Lys-57 is not conserved in human thioredoxin, being replaced by Glu-56, the approximate location of the charge may be conserved with the Lys-39 side chain potentially occupying a similar position (Forman-Kay et al., 1991a). It is unclear, however, how this charge could stabilize a thiolate anion at Cys-32, located over 10 Å away. Regarding the role of Asp-26, stability measurements of oxidized *E. coli* thioredoxin as a function of pH support a thermodynamic linkage of its titration to the stability and redox potential of the *E. coli* protein (Langsetmo et al., 1991). Mutagenesis of Asp-26 to an alanine, however, yields a protein which has retained redox activity (Langsetmo et al., 1990) but whose pH optimum is higher than the one found in the native protein (Eklund et al., 1991), indicative of the intricate nature of the catalytic mechanism.

The recent high-resolution NMR structure of reduced human thioredoxin (Forman-Kay et al., 1991a) provides the first structural argument for the stabilization of the Cys-32 thiolate anion. Cys-32 is located close to the N-terminus of the long second helix, α_2, whose non-hydrogen-bonded amide protons may carry a significant partial positive charge. In particular, the Cys-32 sulfhydryl is ~3 Å away from the Cys-35 amide, which is not involved in a helical hydrogen bond. With distances between the S$^\gamma$ atom of Cys-32 and the NH proton and backbone nitrogen atom of Cys-35 of 2.6 and 3.5 Å, respectively, and an angle between the S$^\gamma$ (Cys-32), the NH (Cys-35) and the N (Cys-35) of 154° in the restrained minimized mean structure, the geometry fits that observed for hydrogen bonds involving sulfur in a survey of proteins in the structure data base (Gregoret et al., 1991). Thus, the positive charge of the helix dipole at the amide of Cys-35 stabilizes the negative charge of the thiolate anion, required for catalysis. This view of the helix dipole as a localized charge at a specific non-hydrogen-bonded amide may provide a more realistic picture of the electrostatics within a helix.

In order to test this partial model for the mechanism of thioredoxin redox function and to better understand the electrostatic behavior of the entire protein, 2D ^{1}H–^{1}H and ^{1}H–^{15}N NMR experiments were performed on reduced human thioredoxin as a function of pH, encompassing the range from pH 2.1 to 10.6. The resulting titration curves were analyzed by a nonlinear least-squares fitting procedure to simple models for the relationship between the ionization constants and the chemical shifts, assuming negligible structural perturbations. Values for the pK_as of a number of isolated carboxyls of aspartic and glutamic acids, as well as for Cys-32, Cys-35, and His-43, were obtained. Although much of the titration data for human thioredoxin are extremely complex, the pK_a values of the active site cysteines (Cys-32 and Cys-35) support the proposed mechanism of thioredoxin catalysis by initial nucleophilic attack of the Cys-32 thiolate anion.

Experimental Procedures

Sample Preparation for NMR Experiments. Natural abundance and uniformly (>95%) ^{15}N-labeled human thioredoxin was purified as described previously (Forman-Kay et al., 1990, 1991a). For simple 1D ^{1}H NMR experiments, 0.2 mM samples of natural abundance human thioredoxin with 0.5 mM dithiothreitol (DTT) and 20 mM sodium phosphate buffer in D_2O were used. Five samples were prepared at pH values of 4.0, 5.0, 5.5, 7.0, and 8.5, sealed, and argon blanketed for 30 min. Approximately 80% of the molecules in this sample retained the N-terminal methionine, due to inefficient posttranslational processing (Forman-Kay et al., 1990), leading to a numbering scheme beginning with Met-1. To maintain the protein in a reduced state for the longer 2D experiments in H_2O, over 200-fold excess of fully deuterated DTT was added to the protein solutions under high pH (>8) conditions, and samples were incubated at 37 °C for at least 15 min. The solutions were then dialyzed overnight into argon-purged 50 mM sodium phosphate buffer at pH ~6 with trace amounts of DTT. The protein solutions were lyophilized and redissolved in 90% H_2O/10% D_2O with 10 mM deuterated DTT, resulting in ~75–100 mM sodium phosphate. The pH was adjusted by the addition of small amounts of concentrated HCl or NaOH. Measurements of the pH of the sample were not corrected for deuterium isotope effects and were taken before and immediately after the NMR experiment, with the latter measurement considered the most accurate. These values differed by less than 0.1 pH units for most measurements. Solutions of approximately 2 mM reduced human thioredoxin were used for NMR experiments at pH values of 5.6–10.6, while lower protein concentrations of around 0.2 mM were used for pH values of 2.1–5.2, necessitated by the reduced solubility of thioredoxin at low pH values. The protein samples used for the 2D heteronuclear studies lacked most of the N-terminal methionine due to different bacterial growth conditions, leading to molecules predominantly having an N-terminal Val-2 (Forman-Kay et al., 1990).

NMR Spectroscopy. All experiments were recorded on a Bruker AM600 spectrometer equipped with digital phase shifters and a "reverse"-mode proton probe and processed on an Aspect 3000 computer. The titration curve for the C$^{\epsilon 1}$ proton of the only histidine, His-43, was obtained by simple 1D experiments in D_2O at 40 °C. Amide ^{1}H and ^{15}N chemical shifts for all residues in the protein were measured from a 2D ^{1}H–^{15}N Overbodenhausen correlation experiment recorded in H_2O at 40 °C (Bodenhausen & Ruben, 1980; Bax et al., 1990). Presaturation was used to suppress the water signal. Figure 1 shows four ^{1}H–^{15}N Overbodenhausen experiments of reduced human thioredoxin, two each from samples at ~0.2 and ~2 mM, over the complete pH titration range. The experiments at low protein concentration were recorded in about 6 h, with 1024 t_1 increments of 2K data points collected, while for high concentration samples 40 min was sufficient. Homonuclear Hartmann–Hahn (HOHAHA) experiments using a WALTZ17 mixing sequence (Bax, 1989) between 1.5-ms trim pulses were performed at 40 °C in H_2O, using the time-proportional incrementation method (Redfield & Kuntz, 1975; Bodenhausen et al., 1980; Marion & Wüthrich,

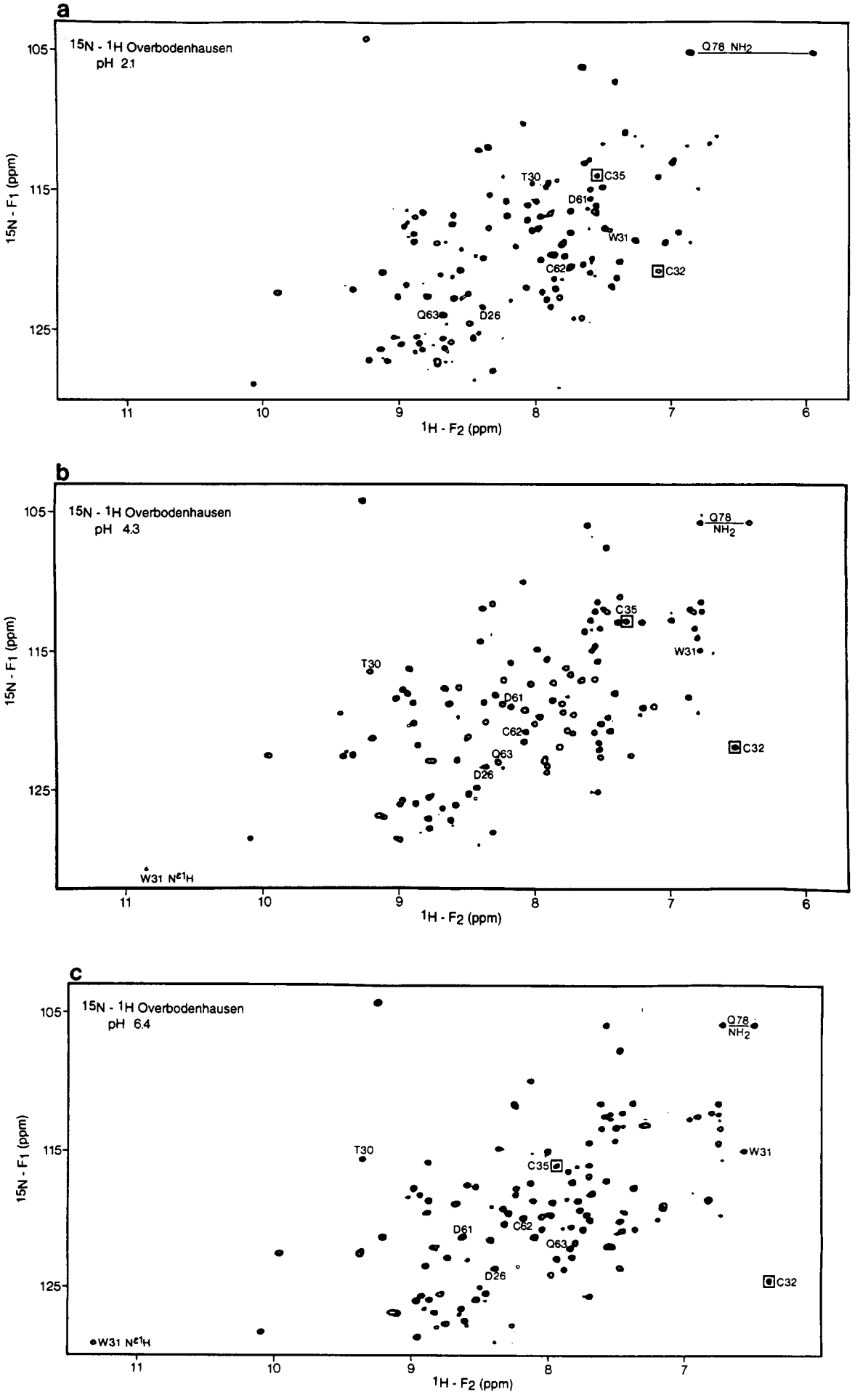
a
15N - 1H Overbodenhausen
pH 2.1
Q78 NH2
T30
C35
D61
W31
C62
C32
Q63
D26
15N - F1 (ppm)
1H - F2 (ppm)
b
15N - 1H Overbodenhausen
pH 4.3
Q78 NH2
C35
W31
T30
D61
C62
C32
Q63
D26
W31 Nε1H
15N - F1 (ppm)
1H - F2 (ppm)
c
15N - 1H Overbodenhausen
pH 6.4
Q78 NH2
T30
W31
C35
D61
C62
Q63
D26
C32
W31 Nε1H
15N - F1 (ppm)
1H - F2 (ppm)

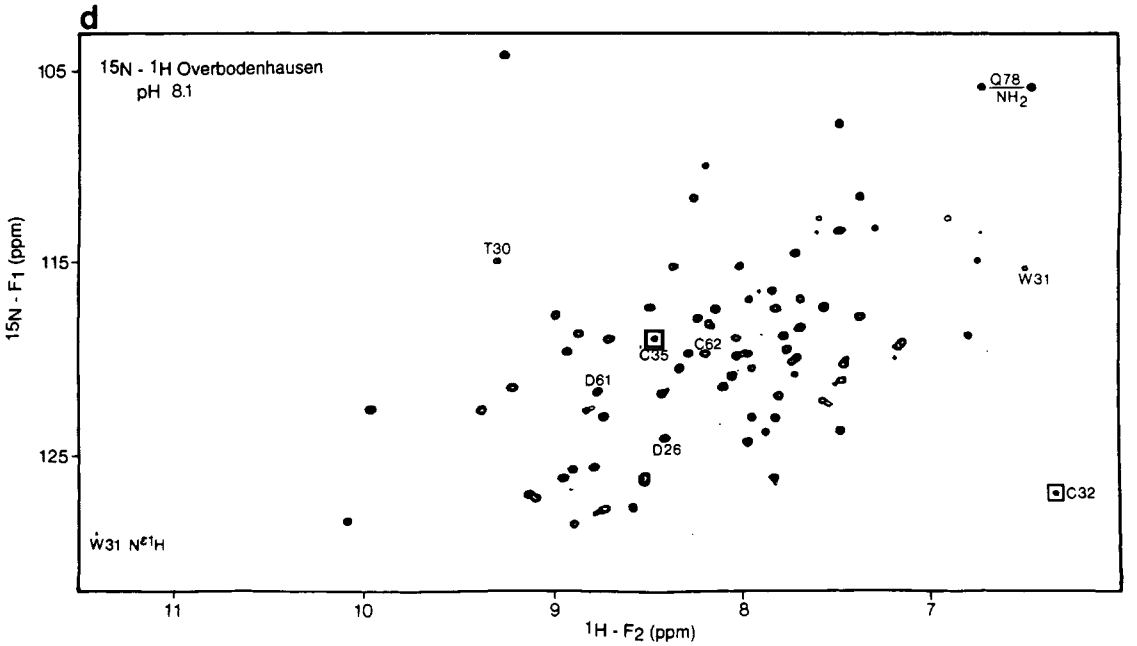

FIGURE 1: ^{15}N (F_1 axis)–NH ^1H (F_2 axis) region of the ^{15}N–^1H Overbodenhausen correlation spectrum of reduced human thioredoxin in H_2O at 40 °C and pH values of 2.1 (a), 4.3 (b), 6.4 (c), and 8.1 (d). Spectra a and b were recorded on samples of ~0.2 mM thioredoxin, while spectra c and d were recorded on ~2 mM samples. Selected ^{15}N–^1H correlation peaks have been labeled, and the active site Cys-32 and Cys-35 peaks are boxed to demonstrate the pH-induced chemical shift changes.

1983) to obtain pure phase absorption peaks. Experiments were recorded in 9 h for high concentration samples and 19 h for those at low concentration, with mixing times of 37–43 ms and 512 t_1 increments of 2K data points. Water suppression involved a 90° "flip-back" pulse, a 100-μs recovery delay, and an on-resonance jump–return pulse sequence following the WALTZ17 mixing sequence (Bax et al., 1987). Figure 2 illustrates two HOHAHA spectra, at pH values of 5.2 and 7.6.

pH Titrations. Heteronuclear ^{15}N–^1H correlation experiments were performed at 26 different pH values between 2.1 and 10.6, the latter value already giving rise to some denaturation. These values were 2.1, 2.2, 2.4, 2.5, 3.2, 3.6, 3.8, 4.3, 4.6, 5.0, 5.2, 5.6, 6.1, 6.4, 6.8, 7.2, 7.5, 7.8, 8.1, 8.4, 8.9, 9.4, 9.8, 10.0, 10.3, and 10.6. HOHAHA experiments were recorded at 23 different pH values of 2.8, 3.2, 3.3, 3.8, 3.80, 4.1, 4.6, 4.7, 5.2, 5.5, 6.2, 6.3, 6.6, 6.7, 7.0, 7.1, 7.6, 7.7, 8.1, 8.2, 8.7, 9.1, and 9.7. The primary goal in recording NH–aliphatic correlations from H_2O HOHAHA spectra was to obtain $C^\alpha H$ and $C^\beta H$ chemical shifts for cysteine and aspartic acid residues, especially Asp-26, and $C^\gamma H$ shifts for glutamic acid residues. The resonance of the downfield $C^\beta Hs$ of Asp-26 completely overlaps the $C^\beta Hs$ of Met-37 at both pH 5.5 and 7.0 in all previous spectra of the aliphatic–aliphatic region, making the more generally useful D_2O HOHAHA or COSY-type experiments inappropriate for extracting the pK_a value for this important residue. Proton chemical shifts were calibrated with respect to the internal ^1H_2O resonance. The chemical shift of ^1H_2O as a function of pH at 40 °C was measured in a series of aqueous solutions of 4 mM sodium trimethylsilylproprionate-d_4 (taken as 0.00 ppm) at eight different pH values. A very small shift of approximately 0.02 ppm was observed between pH 4 and 6, and the proton chemical shift titration curve data were corrected by this amount. Because of the large number of pH values investigated and the resulting smooth titration curves, the resonances in all spectra could be easily assigned by comparison with completely assigned spectra recorded at pH 5.5 and 7.0 (Forman-Kay et al., 1989, 1990).

Calculations of pK_a Values. The large number of pH titration curves were analyzed by multiple fits to a simple model derived from the Henderson–Hasselbalch equation:

$$\text{pH} = \text{p}K_a + \log\{[\text{conjugate base}]/[\text{conjugate acid}]\} = \text{p}K_a + \log(\theta/1-\theta) \quad (1)$$

where θ represents the fractional concentration of the conjugate base. Assuming a rapid equilibrium between protonated and unprotonated forms,

$$\delta = \delta_{base}\theta + \delta_{acid}(1-\theta) \quad \text{and} \quad \theta = (\delta - \delta_{acid})/(\delta_{base} - \delta_{acid}) \quad (2)$$

where δ is the chemical shift of a resonance as a function of pH, and δ_{acid} and δ_{base} represent the chemical shift values at the low and high extremes of pH, respectively. Substituting the relationship for θ as a function of chemical shift into the Henderson–Hasselbalch equation ultimately leads to

$$\delta = [\delta_{acid} + \delta_{base}10^{(\text{pH}-\text{p}K_a)}]/[1 + 10^{(\text{pH}-\text{p}K_a)}] \quad (3)$$

The program FACSIMILE (Chance et al., 1977; Clore, 1983) was used to perform nonlinear least-squares fits of the data to this relationship, with the following three variable parameters: the chemical shifts at the low and high extremes of pH and the pK_a. Data from all chemical shift titration curves of resonances which monitored the titrating group were included, in order to increase the confidence level of the pK_a determination. For situations where many titrating groups could potentially influence one another, fits were made to more than one pK_a (2–7) and up to 50 titration curves were used. A noninteracting model derived as a simple extension of the above relationship was nonetheless sufficient to fit these curves. The resulting general equation for a fit of n different pK_a values, pK_1–pK_n, can be written as

$$\delta = \frac{\sum_{i=0}^{n}\{\delta_i 10^{-[\sum_{j=1}^{n-i}\text{p}K_j + i\text{pH}]}\}}{\sum_{i=0}^{n}\{10^{-[\sum_{j=1}^{n-i}\text{p}K_j + i\text{pH}]}\}} \quad (4)$$

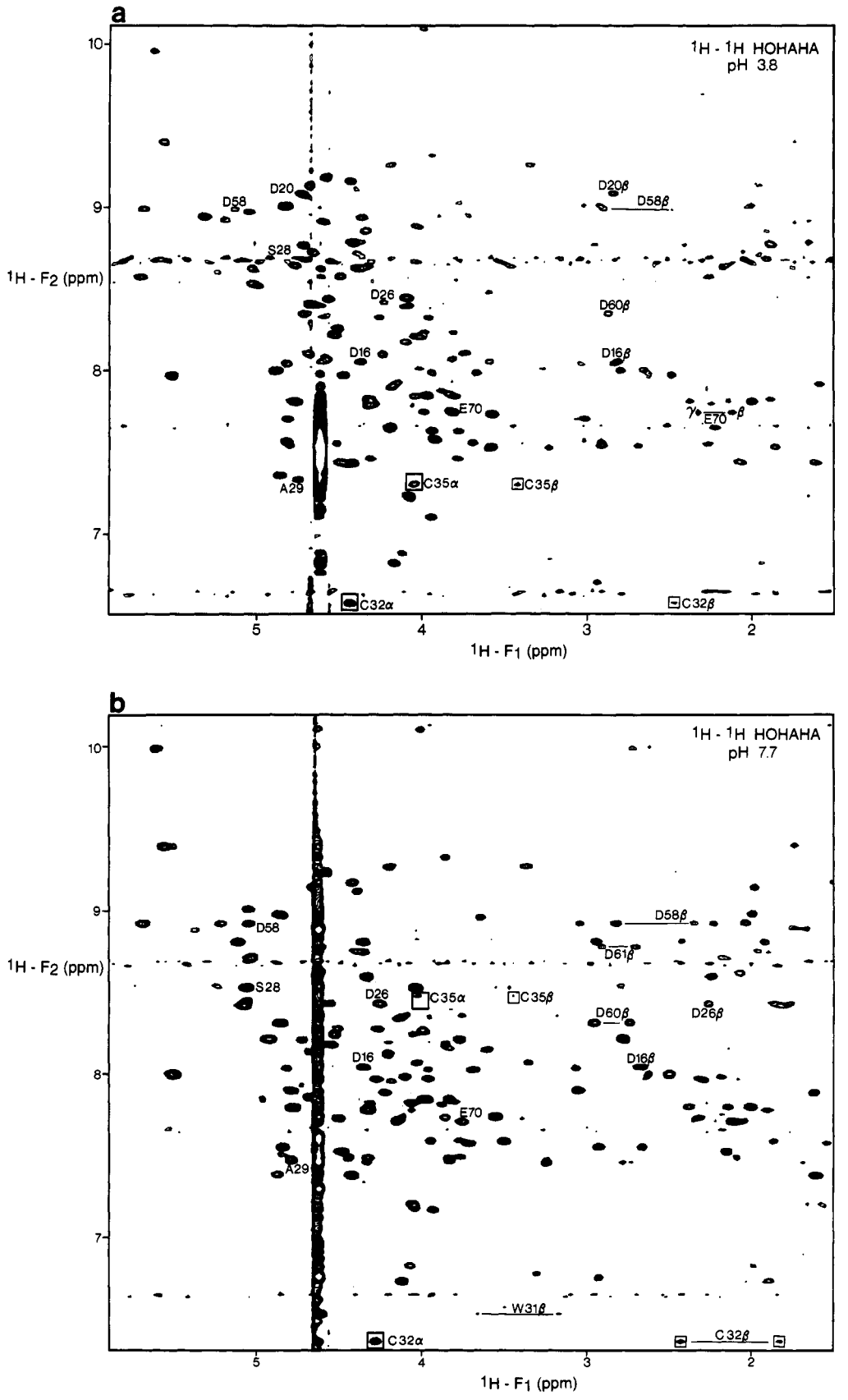

FIGURE 2: NH (F_2 axis)–aliphatic (F_1 axis) region of the 40-ms mixing time HOHAHA spectra of reduced human thioredoxin in H_2O at 40 °C and pH values of 3.8 (a) and 7.7 (b). The concentration of thioredoxin was ~0.2 mM in spectrum a and ~2 mM in spectrum b. Selected peaks have been labeled, and the active site Cys-32 and Cys-35 peaks are boxed.

where $\delta_0 = \delta_{acid}$, $\delta_n = \delta_{base}$, and other δ_i values are intermediate chemical shifts between the pK_as. Even with this simple model, however, there were many variable parameters, including the individual pK_as and the chemical shifts at the intermediate pH values for the titration curve of each resonance. Tests to see if a fit of three pK_as to active site titration curves could

Table I: Largest Observed Chemical Shift Changes for Resonances of Reduced Human Thioredoxin Over the pH Range 2–10

	residue	Δ ppm		residue	Δ ppm
amide ^{1}HN	Thr-30	1.38	amide ^{15}NH	Cys-35	6.2
(≥0.5 ppm)	Asp-61	1.20	(≥5.0 ppm)	Cys-32	6.0
	Cys-35	1.18		Asp-61	5.9
	Trp-31	0.93			
	Gln-63	0.92	side-chain	Trp-31	1.05
	Cys-32	0.72	$N^{\epsilon 1}H$ (≥0.5 ppm)		
	Cys-62	0.50	side-chain NH_2 (≥0.5 ppm)	Gln-78	0.58
aliphatic $C^{\alpha}H$	Asp-61	0.26	aliphatic $C^{\beta}H$	Ala-29	0.41
(≥0.25 ppm)	Ser-28	0.26	(≥0.25 ppm)	Cys-35(b)	0.25

improve with the inclusion of additional parameters for interaction between the pK_as were carried out but resulted in poor determination of the optimized parameters. This indicated that the data did not warrant a model including interaction between the pK_as and led us to apply a noninteracting model in all cases.

Results and Discussion

The ^{1}H and ^{15}N chemical shifts for backbone and side-chain amide groups of reduced human thioredoxin which showed significant titration shifts (greater than ~0.05 ppm in the ^{1}H dimension or 0.5 ppm in the ^{15}N dimension) over the entire pH range were measured from ^{1}H–^{15}N Overbodenhausen correlation experiments. All aliphatic ^{1}H chemical shifts of aspartic and glutamic acids, of the five cysteines, and of residues near the active site region of thioredoxin (Ser-28–Trp-31) were tabulated from the NH–aliphatic cross peaks in HOHAHA experiments. The large amount of data collected can be grouped as follows: ^{1}H chemical shift titration curves were obtained for 86 backbone amides and partial data for six pairs of side-chain amino NH_2 groups (26 pH values) and for 26 C^{α}Hs, 10 degenerate C^{β}Hs, 16 pairs of nondegenerate C^{β}Hs, two degenerate C^{γ}Hs, partial data for five pairs of nondegenerate C^{γ}Hs, and the single $N^{\epsilon 1}$H of Trp-31 (23 pH values), yielding a total of 175 titration curves. One-dimensional data at four pH values and 2D data from the HOHAHA at six different pH values resulted in a titration curve for the His-43 $C^{\epsilon 1}$H of both the N-met and N-Val forms of the protein, covering the interval from pH 4.0 to 8.5. ^{15}N chemical shifts from 60 backbone amides, three side-chain NH_2 groups, and the one $N^{\epsilon 1}$ of Trp-31 were also measured at 26 pH values, leading to 64 additional titration curves. For residues having duplicated resonances due to the N-Met(±) heterogeneity, chemical shifts were measured for both peaks where possible. For the amide groups, the increase in the exchange rate at higher pH values resulted in the loss of some resonances even before reaching the denaturation pH. For most aspartic and glutamic acid residues, chemical shifts of aliphatic protons were only measured at pH values of 7.1 or less.

A qualitative assessment of the amide data reveals that the largest titration shifts occur in the active site region, from residues Thr-30 to Cys-35 and between residues Asp-61 and Gln-63. The largest titration shifts for aliphatic protons are also located within the active site between Ser-28 and Cys-35 and at residue Asp-61. A summary of these observed values is listed in Table I. The observation that the amide proton and nitrogen chemical shifts are the most sensitive to changes in the electronic environment due to changes in the pH may be explained by the fact that the amide N–H bond is much easier to polarize than the C–H bond. Since they are more sensitive, leading to greater chemical shift changes over the pH range, the data measured from these ^{15}N–^{1}H correlation

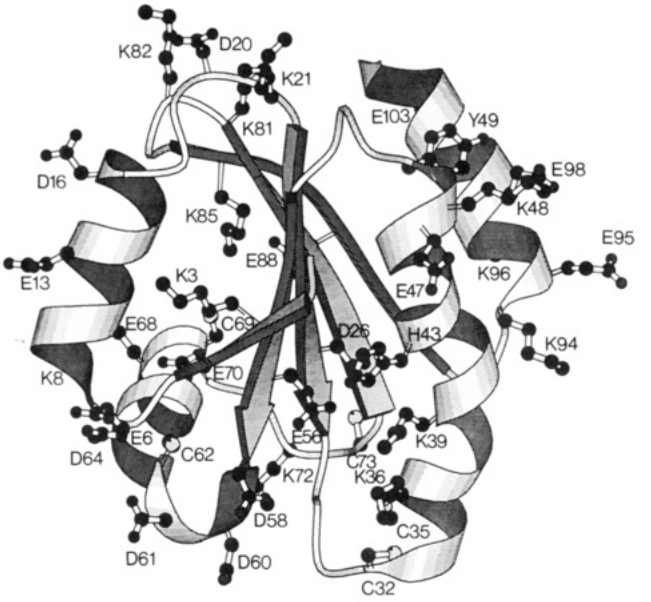

FIGURE 3: Ribbon drawing representation of the solution structure of reduced human thioredoxin illustrating the location of the titrating groups. The structure is from Forman-Kay et al. (1991a), and the ribbon drawing was created with the program MOLSCRIPT (Kraulis, 1991).

experiments have smaller relative errors and yield a more accurate picture of the electrostatic behavior of the protein. The unfortunate aspect of this sensitivity, though, is that due to the apparently low dielectric within the protein core, changes in partial charges can affect resonances over long distances.

For each of the 38 potentially titrating groups in reduced human thioredoxin, a set of titration curves for resonances of nuclei close in space to the chemical group was chosen to be included in the fit to generate its ionization constant. The potentially titrating groups include seven aspartic (16, 20, 26, 58, 60, 61, 64) and 10 glutamic (6, 13, 47, 56, 68, 70, 88, 95, 98) acids, one C-terminal carboxylate, five cysteines (32, 35, 62, 69, 73), one tyrosine (49), one histidine (43), 12 lysines (3, 8, 21, 36, 39, 48, 72, 81, 82, 85, 94, 96), and one N-terminal amino group. The location of these titrating groups on a ribbon drawing representation of the structure of reduced thioredoxin is shown in Figure 3. In the case of some of the surface-exposed and isolated carboxylate groups, the data provided clear answers. For lysine residues and the single tyrosine, however, no accurate ionization constants could be obtained, due to their high pK_as close to the denaturation pH, as well as the loss of signal due to rapidly exchanging amide protons. There was no evidence, however, for any anomalous low pK_as of these groups. For many of the other groups, the interaction of other nearby titrating species and the effects of long-range electrostatic interactions from partially buried charges led to complications in the determination of the pK_a or an inability to assign any pK_a value unambiguously. Very small chemical shift changes over the titration range also prevented our determination of pK_a values for a number of residues. Many of these difficulties were especially apparent in the attempt to understand the titrating behavior of groups within the active site, including Asp-26, which has attracted considerable attention regarding its potential role in redox catalysis by thioredoxin (Langsetmo et al., 1990, 1991a,b; Dyson et al., 1991).

Unambiguous results were obtained for the one histidine and for some aspartic and glutamic acid carboxylate groups. The titration curve observed for the $C^{\epsilon 1}$H of His-43 (Figure 4) exhibits simple Henderson–Hasselbalch behavior and yields

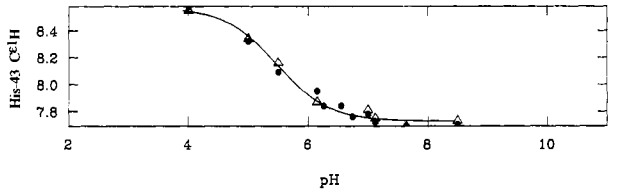

FIGURE 4: His-43 $C^{\epsilon 1}H$ titration curve as a function of pH. Data points were taken from both 1D and 2D HOHAHA spectra of thioredoxin, including resonances of the N-Met (●) and N-Val (△) forms which show identical titration behavior. The solid line is the least-squares best fit to the data derived from resonances of both forms, demonstrating a pK_a of 5.5 ± 0.1.

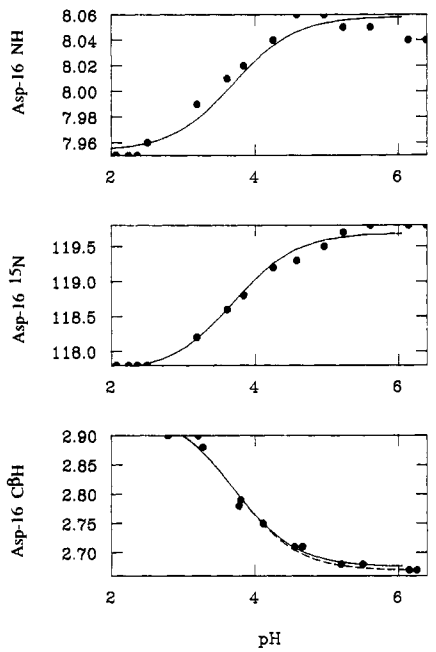

FIGURE 5: Chemical shift titration curves for amide and aliphatic resonances of Asp-16, showing data from both ^1H–^1H HOHAHA and ^1H–^{15}N Overbodenhausen spectra. The solid lines show the least-squares best fit to the data in the pH range of 2–6, demonstrating a pK_a of 3.7 ± 0.1, while the dashed line shows the individual fit to the $C^{\beta}H$ resonance with the identical pK_a of 3.7 ± 0.1.

a pK_a of 5.5 ± 0.1. The $C^{\epsilon 1}H$ resonances from both the N-Met and N-Val form showed identical titration behavior, so the fit included both curves. Similar simple curves were observed for Asp-16 (pK_a = 3.7 ± 0.1) and Asp-20 (pK_a = 3.6 ± 0.1). The pK_as for these ionizable groups were derived from fits of titration curves for resonances of the $C^{\beta}H$s and the amide group of the residue, in order to allow a better determination of the value by using the higher quality amide data. Figures 5 and 6 illustrate the chemical shift titration curve data and the best fit curves (solid lines) calculated by fitting eq 3 to the data for resonances of Asp-16 and Asp-20. For the Asp-16 $C^{\beta}H$ resonances and Asp-20 resonances, individual fits to each titration curve (dashed lines) are superimposed on the fit including all resonances of the residue. In all cases, the individual fits yielded the same pK_a value as those involving multiple titration curves. Both Asp-16 and Asp-20 have 80% or more solvent-exposed surface (Forman-Kay et al., 1991a). While they may be influencing each other, due to their location across an α-helical turn, and Asp-16 may also interact with Glu-13, overall the curves are dominated by a single titration. The pK_a of Glu-13 seems to be 4.8 ± 0.2, as demonstrated by a fit to the aliphatic and ^{15}N amide resonance of this residue. Amino group resonances of two glutamine NH_2s also reflect single titrations of interacting carboxylate groups, with those

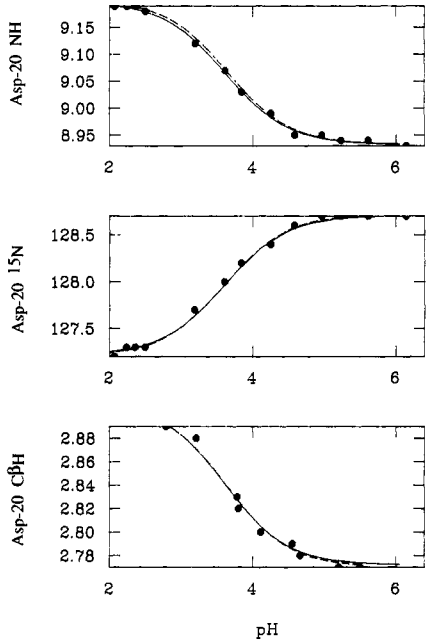

FIGURE 6: Chemical shift titration curves for amide and aliphatic resonances of Asp-20, showing data from both ^1H–^1H HOHAHA and ^1H–^{15}N Overbodenhausen spectra. The solid lines show the least-squares best fit to the data in the pH range of 2–6, demonstrating a pK_a of 3.6 ± 0.1, while the dashed line shows the individual fit to the titration curve of each resonance with pK_as of 3.6 ± 0.1 for the amide NH and ^{15}N curves and 3.6 ± 0.2 for the $C^{\beta}H$ curve.

of Gln-12 monitoring the titration of Asp-16, one helical turn away, and those of Gln-78 monitoring an unassigned titration with a pK_a of 3.4 ± 0.1, possibly Glu-88.

The active site Cys-32 and Cys-35 $C^{\alpha}H$, $C^{\beta}H$, and NH resonances also demonstrate relatively straightforward titration curves with a dominant pK_a of 6.3 ± 0.1 (Figure 7). This value is very close to the pK_a of 6.4 observed in a tryptophan fluorescence study of *E. coli* thioredoxin (Reutimann et al., 1981). A reasonable assignment of this pK_a is to the side-chain sulfhydryl of Cys-32. Since the S^{γ} of Cys-32 is in hydrogen-bonding distance to the amide of Cys-35 (Forman-Kay et al., 1991a), these amide resonances should be among the most sensitive of all protein resonances to the titration of the Cys-32 sulfhydryl. This is confirmed by the extremely large shifts of 1.18 and 6.62 ppm for the ^1H and ^{15}N resonances of Cys-35, respectively. Although the amide resonances of Cys-32 also appear to monitor the same titration, the extent of the chemical shift change is less (see Table I). Numerous other active site resonances demonstrate the effects of a pK_a around 6.3 as well, including the $C^{\beta}H$s of these two cysteines and other resonances from Ser-28 to Ile-38. An additional lower pK_a value is also evident in these curves, at or below ~3, reflecting the titration of another unassigned carboxylate, perhaps Asp-58, Asp-60, or Asp-61.

Many of the titration curves, however, do not demonstrate simple Henderson–Hasselbalch behavior. The interaction of multiple titrating groups gives rise to curves which are quite difficult to interpret in terms of a single or a few distinct pK_a values, and the effects of partial charges at long distances through the protein interior makes assignment of any resulting pK_as ambiguous. In addition, chemical shift perturbations due to changes of conformation are superimposed on the shift changes resulting from the titrations of interest. In order to extract the major pK_a from these complicated curves, a simplified approach was taken. Data from titration curves of both amide and aliphatic resonances of a titrating residue were simultaneously fit to a Henderson–Hasselbalch curve (eq 3).

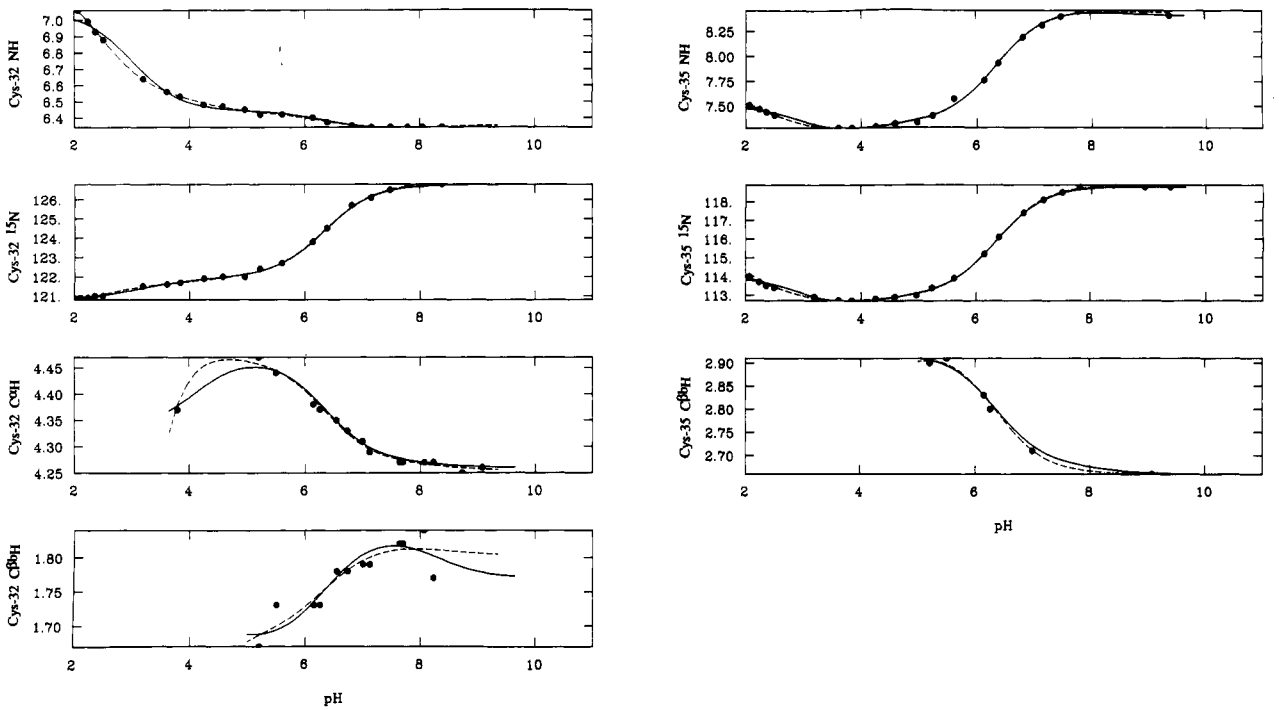

FIGURE 7: Chemical shift titration curves for the active site amide and aliphatic resonances of Cys-32 and Cys-35, with data from both ^{1}H–^{1}H HOHAHA and ^{1}H–^{15}N Overbodenhausen spectra. The solid lines show the least-squares best fit to 28 titration curves from the active site region (identified in the text), demonstrating four pK_as of 3.0 ± 0.1, 4.1 ± 0.1, 6.3 ± 0.1, and 8.2 ± 0.3. The dashed lines illustrate a fit to the seven plotted resonances of the active site cysteine residues, yielding pK_as of 2.4 ± 0.2, 4.2 ± 0.4, 6.3 ± 0.1, and 8.4 ± 1.3.

Although the experimental curves showed deviations from these simple fits, the results provide qualitative information about the pK_as of certain ionizable groups of human thioredoxin. Asp-64 appears to have a pK_a of 3.1 ± 0.2, although it is close to a cluster of other aspartic acid residues including Asp-58, Asp-60, and Asp-61 and has a relatively low surface accessibility of 20%, giving rise to titration curves which are influenced by multiple pK_as. Glu-68 and Glu-88 exhibit a midpoint of their titration curves at 4.2 ± 0.2 and 3.9 ± 0.2, respectively, but they clearly show the effects of other lower pK_as. With the large number of negatively charged residues in human thioredoxin, this is not surprising. These pK_as of carboxyl groups are also near the values of 4.0 for aspartic acid and 4.4 for glutamic acid side chains seen in denatured proteins (Nozaki & Tanford, 1967).

In an effort to analyze the large amount of data which were collected and to derive more meaningful results regarding the electrostatic behavior of thioredoxin, the ionizable residues within the molecule were grouped into potentially interacting groups. The experimental data were simultaneously fit to ionization constants for each of the involved titrating side chains, with two to seven pK_as using eq 4. These calculations included titration curves of many resonances, which appeared to be monitoring not only the pK_as of interest in the interacting group but other pK_as as well. The results of these multiple fits, though, did not yield pK_as which could be unambiguously assigned to single side-chain groups, although in some cases general trends could be inferred.

The set of ionizable groups on which most of our effort was focused comprised those within the active site (Figure 3). This contains an overabundance of potentially charged residues, including two Cys-32 and Cys-35 sulfhydryls, Glu-56, Asp-26, Asp-58, Asp-60, and Asp-61 carboxylates, Lys-36 and Lys-39 N$^{\zeta}$H$_3$ groups, and the His-43 imidazole ring. In addition, many of these side chains are relatively surface inaccessible, especially Asp-26, Glu-56, Asp-58, and the two active site cysteines. Multiple calculations were performed, fitting different groups of chemical shift curves over various pH regions to equations involving anywhere from one to seven pK_as. All of the results exhibited midpoints of titration at pH 6.1–6.4, corresponding to the pK_a value of 6.3 ± 0.1 extracted from a simple fit of eq 3 to only Cys-32 and Cys-35 resonances. A fit involving 28 titration curves from active-site resonances (Ser-28 C$^{\alpha}$H, C$^{\beta a}$H, C$^{\beta b}$H; Ala-29 NH, ^{15}N, C$^{\alpha}$H, C$^{\beta}$H; Thr-30 NH, ^{15}N; Trp-31 NH, ^{15}N, N$^{\epsilon 1}$H, ^{15}N$^{\epsilon 1}$; Cys-32 NH, ^{15}N, C$^{\alpha}$H, C$^{\beta a}$H, C$^{\beta b}$H; Cys-35 NH, ^{15}N, C$^{\alpha}$H, C$^{\beta a}$H, C$^{\beta b}$H; Lys-36 NH, ^{15}N; Met-37 NH, ^{15}N; Thr-74 NH) revealed multiple pK_as of 3.0 ± 0.1, 4.1 ± 0.1, 6.3 ± 0.1, and 8.2 ± 0.3, showing the influence of a number of ionizable groups in this region. The resulting best fit curves to the Cys-32 and Cys-35 titration curves are shown as solid lines in Figure 7. Another fit involving only the resonances of the two active site cysteine residues (Cys-32 NH, ^{15}N, C$^{\alpha}$H, C$^{\beta b}$H; Cys-35 NH, ^{15}N, C$^{\beta b}$H) is also illustrated, with a dashed line. This fit yielded similar pK_as of 2.4 ± 0.2, 4.2 ± 0.4, 6.3 ± 0.1, and 8.4 ± 1.3. The titration observed at pH 8.2–8.4 could tentatively be assigned to the Cys-35 sulfhydryl. This pK_a value was not very well determined, however, since variation between many different fits were noticed, clustering around 7.5–8.6, but even exhibiting values of 7.1–9.2 in others. This pK_a does correspond, though, to one around 8.5–9.0 measured in previous biochemical and NMR studies of *E. coli* thioredoxin (Kallis & Holmgren, 1980; Dyson et al., 1991). More specific assignments of the low and high pK_as could not be made beyond attributing them to one or more of the three aspartic acids and one or both of the two lysines. The average percentage of the chemical shift changes for the seven Cys-32 and Cys-35 resonances plotted in Figure 7 attributable to each of the pK_as is as follows: pK_a 2.4 (16%), pK_a 4.1 (12%), pK_a 6.3 (63%), and pK_a 8.4 (8%). The dominance of the Cys-32 titration at pH 6.3 is evident. Note that no pK_a around 5.5 was detected in the fits, showing that the titration of His-43 is independent of these other ionizations, allowing the determination of its pK_a solely from analysis of the C$^{\epsilon 1}$H chemical

shift curve and effectively eliminating it from consideration in terms of redox function.

The C-terminal carboxylate of thioredoxin was included in a group with the side chain of Glu-103 (Figure 3). Fits to two pK_as resulted in values of 3.2 ± 0.1 and 4.9 ± 0.1 for the C-terminus and Glu-103, respectively. These tentative assignments were made on the basis of the closer fit of the titration of the Glu-103 C$^\gamma$Hs to the higher pK_a value and on the basis of reference pK_a values of 4.4 for glutamic acids and 3.8 for the C-terminus. The α-amino group of the N-terminal Val-2 was analyzed as a separate, noninteracting ionization. A titration of 7.3 ± 0.2 was observed, equal to the reference pK_a of 7.5 for α-amino groups. The fact that this pK_a is so close to neutral suggests a possible cause for the dramatic duplication of a third of the backbone resonances of reduced thioredoxin caused by the N-terminal heterogeneity (Forman-Kay et al., 1990). If the pK_a of the N-terminal Met-1 α-amino group is even slightly shifted from the value observed for Val-2, a localized partial charge difference might explain the duplications in chemical shift for resonances spread over the whole face of the protein. Alternatively, the movement of the charge could also explain these chemical shift changes, even with no difference in pK_a.

The three additional cysteines of human thioredoxin are also found within close range of each other (Figure 3). No evidence for titrations within this clustered group of cysteines was found, however. The amide proton of Cys-73 exchanges too rapidly to be seen much above pH 7, while the very small shifts for the resonances of Cys-62 and Cys-69 were not sufficiently reliable to extract pK_a values. These latter two cysteine residues may well remain protonated up to pH values close to the denaturation pH of the protein, since both sulfhydryl groups are less than 10% surface accessible. The accessibility of Cys-73 is greater, though, at approximately 60%.

Another group of interacting charges was studied, comprising the six potential salt bridges identified within the solution structure of reduced human thioredoxin (Forman-Kay et al., 1991a). These are between the carboxylate group of Asp-20 and the N$^\zeta$H$_3^+$ groups of Lys-81 or Lys-82, Glu-56 and Lys-36 or Lys-39, Glu-68 and Lys-8, Glu-88 and Lys-85, Glu-95 and Lys-94, and Glu-98 and Lys-48 (Figure 3). None of the fits were conclusive in determining whether an interaction between the charges could stabilize the potentially buried charge of Glu-56 or if these interactions led to anomalous pK_a values. A simple fit to the Glu-56 C$^\gamma$Hs is also not convincing due to the extremely small changes in chemical shifts observed across the entire pH range (0.01 and 0.04 ppm).

Other potentially buried charges are located with the extended active site region, including Asp-26 and Asp-58 (Figure 3). The solution structure identifies possible stabilizing interactions for Asp-26 with the O$^\gamma$H of Ser-28 and for Asp-58 with the main-chain carboxyls of Thr-30, Asp-60, and Asp-61 (Forman-Kay et al., 1991a). In addition, a study of the structure of bound water in reduced human thioredoxin reveals a water located in close proximity to the Asp-26 side chain (Forman-Kay et al., 1991b). The fits of the entire active site do not reveal any specific information about these groups, but the individual fits suggest a pK_a of 3.1 ± 0.2 for Asp-58, although the effects of a probable interaction with the Asp-60 and Asp-61 pK_as on this value cannot be ignored. Asp-26 is much more complex, showing multiple pK_as within the titration curves for the resonances of this residue (Figure 8), but with overall little change in chemical shift, especially for the C$^\beta$Hs (0.06 ppm). A major titration overlaps the active site pK_a of 6.3, with two inflections in the acidic pH range around 3 and

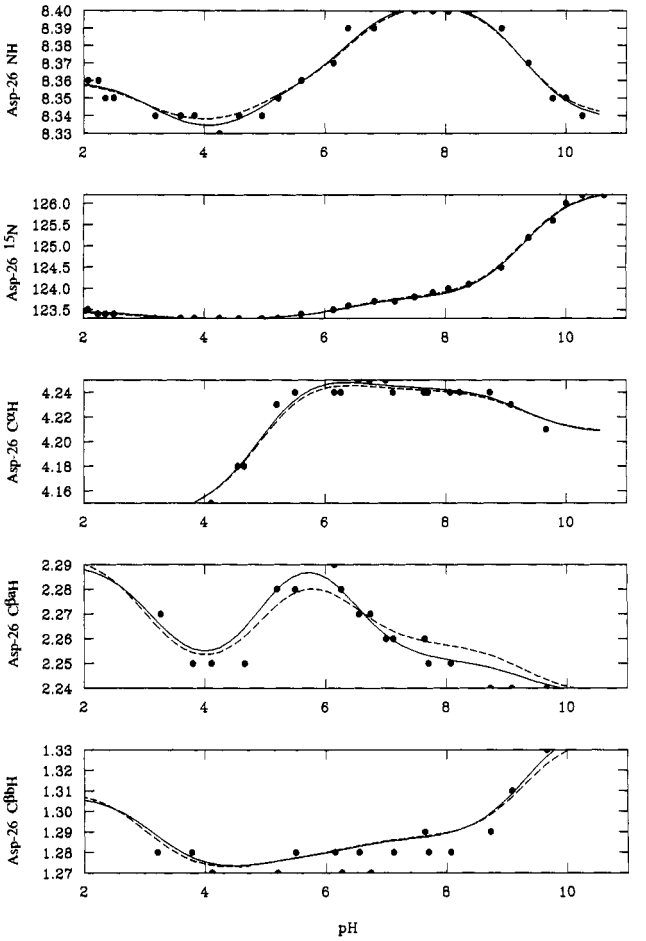

FIGURE 8: Chemical shift titration curves for amide and aliphatic resonances of Asp-26, with data from both ^{1}H–^{1}H HOHAHA and ^{1}H–^{15}N Overbodenhausen spectra. The solid lines show the least-squares best fit to 16 titration curves of resonances (identified in the text) that monitor the buried Asp-26 and Glu-56 carboxylate groups, demonstrating four pK_as of 3.2 ± 0.3, 5.0 ± 0.4, 6.4 ± 0.1, and 9.3 ± 0.1. The dashed lines illustrate a fit to data from the five Asp-26 resonances, with pK_as of 3.2 ± 0.9, 5.0 ± 0.4, 6.4 ± 0.3, and 9.3 ± 0.1.

5 (near the His-43 C$^{\epsilon 1}$H titration). A fit involving 16 titration curves monitoring the buried Asp-26 and Glu-56 carboxylate groups (Asp-26 NH, ^{15}N, C$^\alpha$H, C$^{\beta a}$H, C$^{\beta b}$H; Ser-28 NH, ^{15}N, C$^\alpha$H, C$^{\beta a}$H, C$^{\beta b}$H; Thr-30 C$^\beta$H; Glu-56 NH, ^{15}N, C$^\alpha$H, C$^\beta$H, C$^{\gamma b}$H), shown as a solid curve, led to pK_as of 3.2 ± 0.3, 5.0 ± 0.4, 6.4 ± 0.1, and 9.3 ± 0.1. These values agree with those derived from a fit using only the five resonances observed for Asp-26, 3.2 ± 0.9, 5.0 ± 0.4, 6.4 ± 0.3, and 9.3 ± 0.1. These fits are plotted as dashed curves. These patterns observed for the Asp-26 titration curves of human thioredoxin are markedly different from those seen in the NMR study of the reduced *E. coli* protein (Dyson et al., 1991), where a significant titration shift (~0.2 ppm) of one of the C$^\beta$Hs was observed with a pK_a of 7.2–7.3.

The basically unperturbed chemical shift (≤0.06 ppm) of the Asp-26 C$^\beta$Hs in reduced human thioredoxin as a function of pH (range: 2.1–10.6) can most readily be explained by assuming that the side-chain carboxyl is always protonated, as perhaps expected in its relatively buried position, or, less likely, that the effects of other ionizable groups or conformational changes are masking the intrinsic titration of the Asp-26 carboxyl. Since the average chemical shift change of the measured C$^\beta$Hs of aspartic acid residues in this study is only 0.10 ± 0.07, however, this small chemical shift change may not be a clear diagnostic for a stable protonated state over

the entire pH range. A similar argument could hold for the buried Glu-56 being protonated at physiological pH, since the changes in chemical shift over the measured pH range (2.8–7.1) for the two C^{γ}Hs are only 0.01 and 0.04 ppm. The average chemical shift change for measured C^{γ}Hs of glutamic acid residues, however, is also not large (0.07 ± 0.06). The possibility exists that the pK_a of Asp-26 is one of the values involved in the fits described above (3.3, 5.0, 6.3, or 9.0), but an equally likely possibility is that these values reflect the titrations of other groups within the protein monitored by Asp-26 resonances.

In interpreting any of these titration data, the relationship between the chemical shift and electrostatics must be addressed. The analysis of pK_as relies on a macroscopic view of the system, since at any one time an ionizable group is either protonated or deprotonated. The chemical shift of a given resonance results from the averaging of the NMR frequencies from two different conformational states in rapid equilibrium, one in which a proton is bound and one in which it is ionized. The resonance frequency of a nucleus in the individual states is due to its electronic shielding. The dominant effects on the chemical shift are the electronegativity of and partial charge on atoms which are covalently bound, since these have an immediate influence on the polarization of the electrons surrounding the nucleus observed in the NMR experiment. Other important effects on the chemical shift can be attributed to the relative position of the nucleus to charges on ionizable groups and π-shell aromatic electrons and to the collective charge potential of all electrons of the protein in the given conformational state. The changes in chemical shift over the pH range are caused by a shift in the equilibrium from a situation favoring the protonated states of titrating groups to one favoring the deprotonated states. The conformational change required to accommodate or lose a proton may in some cases be extemely small or may in certain situations be more significant. Thus, the change in chemical shift may be attributed primarily to a change in the local charge density near an ionizable group, especially on a covalently bound atom, or to a conformational change accompanied by a change in the overall electric potential.

There are other difficulties in interpreting these pH titration curves in terms of the biochemical mechanism of thioredoxin catalysis. For example, it is possible for more than one group to ionize within what appears to be a single observed titration shift. Therefore, it is difficult to separate and individually assign very close pK_as. The overall results of these experiments, though, do correlate with the current understanding of thioredoxin catalysis as well as with previous measures of pK_as within the active site (Kallis & Holmgren, 1980; Reutimann et al., 1981).

Having determined these experimental pK_a values, it would be instructive to compare our results with those predicted by electrostatic theory. Computational algorithms for this purpose are still in a developmental stage, with some limited success in predicting pK_as of titrating groups in proteins (Bashford & Karplus, 1990). Their primary application, however, may not be in predicting pK_as but in aiding the interpretation of observed electrostatic effects. Application of the program DelPhi (Honig et al., 1988) to study the anomalously low pK_a observed for Cys-32, as well as other pK_as derived from these titration experiments, is now under way.

Concluding Remarks

Using 2D ^1H and ^{15}N NMR, a total of 241 chemical shift titration curves as a function of pH were measured. Nonlinear least-squares fits of the data to a simple relationship derived from the Henderson–Hasselbalch equation allowed unambiguous pK_as for certain isolated ionizable groups to be extracted. These include pK_as for the titration of His-43 and a number of aspartic and glutamic acid residues. The values obtained for the most part were close to the reference pK_as of the amino acid side chain. The pK_a value of His-43 (5.5 ± 0.2), however, is significantly shifted to a lower pH value than the reference value of 6.3 (Nozaki & Tanford, 1967), consistent with its limited surface accessibility of about 66%.

The results for titrations within the active site support the model for thioredoxin redox catalysis by initial attack of the thiolate anion of Cys-32. The experimentally observed pK_a of Cys-32 is 6.3 ± 0.1, while that of Cys-35 is probably between 7.5 and 8.6. These values are in agreement with the previously measured pK_as of active site residues of *E. coli* thioredoxin of 6.4–6.8 and 8.5–9.0 from chemical modification and fluorescence studies (Holmgren, 1972; Kallis & Holmgren, 1980; Reutimann et al., 1981) and 7.1–7.4 and 8.4 from NMR analysis (Dyson et al., 1991). The anomalously low pK_a for Cys-32 can be explained by the hydrogen-bonding interaction between its S^{γ} atom and the backbone amide of Cys-35 seen in the solution structure of reduced human thioredoxin (Forman-Kay et al., 1991a), stabilizing the Cys-32 thiolate anion at physiological pH values.

There is no clear evidence for the titration of the Asp-26 carboxylate, and the titration behavior of many of the 38 potentially ionizable groups in thioredoxin, including other groups within the active site, is extremely complex. The effects of nearby interacting titrating groups, long-range interactions through the low dielectric core of the protein, and pH-induced conformational changes on chemical shifts can lead to complicated titration curves which often do not yield unambiguous assignments of pK_as to individual ionizable groups. This study of the pH-induced chemical shift titrations of NMR resonances of the protein, however, has resulted in the determination of the pK_a of Cys-32 and, in conjunction with knowledge from the solution structure of reduced human thioredoxin, has provided a foundation for further analysis of the role of electrostatics in the function of this redox catalyst.

Supplementary Material Available

Titration curve data in the form of a table of chemical shifts as a function of pH for the 241 tabulated resonances (16 pages). Ordering information is given on any current masthead page.

Registry No. Asp, 56-84-8; Glu, 56-86-0; Cys, 52-90-4; Tyr, 60-18-4; His, 71-00-1; Lys, 56-87-1.

References

Bax, A. (1989) *Methods Enzymol. 176*, 151–168.

Bax, A. Sklenar, V. Clore, G. M., & Gronenborn, A. M. (1987) *J. Am. Chem. Soc. 109*, 6511–6513.

Bax, A., Ikura, M., Kay, L. E., Torchia, D. A., & Tschudin, R. (1990) *J. Magn. Reson. 86*, 304–318.

Bashford, D., & Karplus, M. (1990) *Biochemistry 29*, 10219–10225.

Bodenhausen, G., & Ruben, D. J. (1980) *Chem. Phys. Lett. 69*, 185.

Bodenhausen, G., Vold, R. L., & Vold, R. R. (1980) *J. Magn. Reson. 37*, 93–106.

Cantor, C. R., & Schimmel, P. R. (1980) *Biophysical Chemistry*, W. H. Freeman and Co., San Francisco, CA.

Chance, E. M., Curtis, A. R., Jones, I. P., & Kirby, C. R. (1977) FACSIMILE: *A Computer Program for Flow and*

Chemistry Simulation, and General Initial Value Problems, Computer Sciences and Systems Division, AERE Harwell, Oxfordshire.
Clore, G. M. (1983) in *Computing in Biological Science* (Geisow, M., & Barrett, A. N., Eds.) pp 314-348, Elsevier Biomedical Press, Amsterdam.
Dyson, H. J., Gippert, G. P., Case, D. A., Holmgren, A., & Wright, P. E. (1990) *Biochemistry 29*, 4129-4136.
Dyson, H. J., Tennant, L. L., & Holmgren, A. (1991) *Biochemistry 30*, 4262-4268.
Ebina, S., & Wüthrich, K. (1984) *J. Mol. Biol. 179*, 283-288.
Eklund, H., Gleason, F. L., & Holmgren, A. (1991) *Proteins 11*, 13-28.
Forman-Kay, J. D., Clore, G. M., Driscoll, P. C., Wingfield, P. T., Richards, F. M., & Gronenborn, A. M. (1989) *Biochemistry 28*, 7088-7097.
Forman-Kay, J. D., Gronenborn, A. M., Kay, L. E., Wingfield, P. T., & Clore, G. M. (1990) *Biochemistry 29*, 1566-1572.
Forman-Kay, J. D., Clore, G. M., Wingfield, P. T., & Gronenborn, A. M. (1991a) *Biochemistry 30*, 2685-2698.
Forman-Kay, J. D., Gronenborn, A. M., Wingfield, P. T., & Clore, G. M. (1991b) *J. Mol. Biol. 220*, 209-216.
Gleason, F. K., Lim, C.-J., Gerami-Nejad, M., & Fuchs, J. A. (1990) *Biochemistry 29*, 3701-3709.
Gregoret, L. M., Rader, S. D., Fletterick, R. J., & Cohen, F. E. (1991) *Proteins 9*, 99-107.
Holmgren, A. (1972) *J. Biol. Chem. 247*, 1992-1998.
Holmgren, A. (1989) *J. Biol. Chem. 264*, 13963-13966.
Holmgren, A. Söderberg, B.-O., Eklund, H., & Brändén, C.-I. (1975) *Proc. Natl. Acad. Sci. U.S.A. 72*, 2305-2309.
Honig, B., Sharp, K., Gilson, M., Fine, R., & Nicholls, A. (1988) *DelPhi—A Macromolecular Electrostatics Modelling Package*, Columbia University, New York.
Kallis, G. B., & Holmgren, A. (1980) *J. Biol. Chem. 255*, 10261-10265.
Katti, S. K., LeMaster, D. M., & Eklund, H. (1990) *J. Mol. Biol. 212*, 167-184.
Kohda, D., Sawada, T., & Inagaki, F. (1991) *Biochemistry 30*, 4896-4900.
Kraulis, P. J. (1991) *J. Appl. Crystallogr. 24*, 946-950.
Langsetmo, K., Sung, Y.-C., Fuchs, J., & Woodward, C. (1990) in *Current Research in Protein Chemistry: Techniques, Structure, and Function* (Villafranca, J., Ed.) pp 449-456, Academic Press, San Diego, CA.
Langsetmo, K., Fuchs, J. A., & Woodward, C. (1991a) *Biochemistry 30*, 7603-7609.
Langsetmo, K., Fuchs, J. A., Woodward, C., & Sharp, K. A. (1991b) *Biochemistry 30*, 7609-7614.
Marion, D., & Wüthrich, K. (1983) *Biochem. Biophys. Res. Commun. 113*, 967-974.
Nozaki, Y., & Tanford, C. (1967) *Methods Enzymol. 11*, 715-734.
Redfield, A. G., & Kuntz, S. D. (1975) *J. Magn. Reson. 19*, 250-254.
Reutimann, H., Straub, B., Luisi, P. L., & Holmgren, A. (1981) *J. Biol. Chem. 256*, 6796-6803.

Effects of Calcium Binding on the Internal Dynamic Properties of Bovine Brain Calmodulin, Studied by NMR and Optical Spectroscopy†

K. Török, A. N. Lane, S. R. Martin, J.-M. Janot,‡ and P. M. Bayley*
National Institute for Medical Research, Mill Hill, London NW7 1AA, U.K.
Received July 18, 1991; Revised Manuscript Received November 14, 1991

ABSTRACT: The dynamic properties of bovine brain calmodulin have been studied as a function of binding calcium ions, using a number of complementary spectroscopic methods. Rotational correlation times for proton–proton vectors within tyrosine and phenylalanine residues of calmodulin have been determined from time-dependent NOE measurements. In the presence of Ca^{2+}, a range of rotational correlation times is observed. The longest value is consistent with Ca_4–calmodulin having a markedly nonspherical shape in solution. In the absence of Ca^{2+}, the rotational correlation times of all vectors are significantly shorter, indicating that several phenylalanine side chains in apocalmodulin have increased internal dynamics. Time-resolved tyrosine fluorescence anisotropy shows global correlation times broadly in agreement with the NMR results, but with an additional faster correlation time [≈600 ps]. Tyrosine residues in apocalmodulin have substantial segmental motion, which becomes significantly reduced, but not eliminated, when Ca^{2+} is bound. The correlation time for global rotation of Ca_4–calmodulin increases from pH 7 to 4.5, indicating increased overall molecular asymmetry. This occurs without a significant change in total α-helix content as measured by circular dichroism. These results are consistent with the central region of Ca_4-calmodulin being relatively flexible in solution at pH 7, but with the molecule adopting a more extended shape under more acidic conditions. The Ca^{2+}-induced change in α-helix content can be mimicked by protonation. The α-helix content of Ca_4–calmodulin in solution appears less than in the crystal structure; additional α-helix is induced in partially nonaqueous solutions, particularly at acidic pH, as used in crystallization conditions.

Calmodulin is a ubiquitous intracellular Ca^{2+}-receptor protein which in the Ca^{2+}-loaded state can interact with and activate a number of protein kinases [see Klee (1988)]. The crystal structure of calmodulin (Babu et al., 1985, 1988; Kretsinger et al., 1986) shows that the protein consists of two Ca^{2+}-binding domains, each containing two E-F hand motifs, separated by an extended central α-helix to form a dumbbell-like shape. The mammalian protein contains two tyrosine residues but no tryptophan. Conformational changes involving

†The work was supported in part by EC Twinning Grant 852/00255/UK/05/PUJU1 (to P.M.B.) and the National Institutes of Health Grant 15835 to the Pennsylvania Muscle Institute.
*To whom correspondence should be addressed.
‡Present address: CNRS UA 330, 34033 Montpellier, France.

0006-2960/92/0431-3452$03.00/0